HEFAT2011
8th International Conference on Heat Transfer, Fluid Mechanics and Thermodynamics
11 July – 13 July 2011
Pointe Aux Piments, Mauritus

Numerical Investigation of Flow and Heat Transfer in Closed Cavities Partially Heated from Below

Singh S.N
Department of Mechanical Engineering and Mining Machinery Engineering,
Indian School of Mines Dhanbad
Dhanbad- 826004
India
E-mail: snsingh63@yahoo.com, singh.sn.memme@ismdhanbad.ac.in

ABSTRACT
The present problem deals with the numerical study of two-dimensional, steady, incompressible, laminar natural convection in air filled cavity with a centrally heated bottom wall and cooled upper wall. The vertical walls and the rest of the bottom walls are assumed to be insulated. Results are presented for Ra = 10^3 - 3×10^6, A = 1-3, W = 0.25 - 1 and Pr = 0.7. The governing equations, written in terms of stream-function-vorticity formulation, are solved using a finite volume method. The influence of heated surface dimension on the fluid flow and thermal patterns is also presented by comparing the present results against those obtained by the author in an earlier study within a square cavity heated from below. Based on numerical data a correlation has been developed for convective heat transfer.

INTRODUCTION
Natural convection flows caused by buoyancy forces occur in many thermal engineering systems, such as solar energy efficient buildings, double-pane windows, cooling of electronic equipment and so forth. Despite significantly lower values of heat transfer coefficient, cooling by natural convection using air is preferred, for example, in numerous electronic cooling applications because of its low cost, inherent reliability, simplicity and noiseless method of thermal control.

To date, many experimental and numerical studies have been conducted on the natural convection heat transfer in the rectangular closed cavities. Most of the numerical studies previously reported in the literature have considered one of the vertical walls heated and the other one cooled with horizontal insulated walls. Excellent reviews of laminar natural convection have been presented by Ostrach [1] and Hoogendoom [2]. Benchmark numerical solutions for natural convection in a square enclosure with two isothermal and two adiabatic walls have been obtained by de Vahl Davis and Jones [3]. Akiyama and Chong [4] studied the problem for coupled natural convection and radiation in a square enclosure filled with air and having gray surfaces. Using the finite volume method, Mezrhab and Behir [5] studied the heat transfer by radiation and natural convection in an air-filled square enclosure with a vertical partition of finite thickness and varying height. Mahapatra et al. [6] reported a finite element solution on the interaction of surface radiation and variable property laminar natural convection in a differentially heated square cavity. Colomer et al. [7] analyzed the natural convection phenomenon coupled with radiant heat exchange in a three –dimensional differentially heated cavity.

NOMENCLATURE

A	[-]	aspect ratio, H'/L'
g	[m/s^2]	acceleration due to gravity
Gr	[-]	Grashof number
H', L'	[m]	height and width of the cavity
m	[-]	number of grid points in horizontal direction
n	[-]	number of grid points in vertical direction
Nu_c	[-]	convection Nusselt number
$\overline{Nu}_C$	[-]	average convection Nusselt number
Pr	[-]	Prandtl number, ν/α
Ra	[-]	Rayleigh number, Gr × Pr
T	[°C]	variable temperature at any wall
T_h	[°C]	temperature at centrally heated boundary
u	[m/s]	vertical velocity
U	[-]	dimensionless vertical velocity, uL'/α
v	[m/s]	horizontal velocity
V	[-]	dimensionless vertical velocity, v L'/α
w	[m]	centrally heated bottom part
W	[-]	heated bottom part ratio, w/H'
x	[m]	vertical coordinate

X	[-]	dimensionless vertical coordinate, x/H'
y	[m]	horizontal coordinate
Y	[-]	dimensionless horizontal coordinate, y/H'

Subscripts

c	convection
h	hot
i,j	number of variables of nodal points in Y and X directions respectively.
∞	ambient

Greek symbols

α	[m^2/s]	fluid thermal diffusivity, m^2/s
ν	[m^2/s]	kinematic viscosity of fluid
θ	[-]	dimensionless temperature, $(T- T_\infty)/(T_h - T_\infty)$
ψ'	[m^2/s]	stream function,
ψ	[-]	dimensionless stream function, ψ'/α
ω'	[1/s]	vorticity
ω	[-]	dimensionless vorticity, $\omega' H'^2/\nu$

When the heating/cooling scenario switches from vertical to horizontal walls, Hasnaoui et al. [8] have demonstrated numerically the existence of multiple steady-state solutions in the absence of radiation in a rectangular cavity partially heated from below. Recently, while studying coupling between radiation and natural convection in a square cavity entirely heated from below, Ridouane et al. [9, 10] demonstrated also that the multiplicity of solutions is possible. Recently, Ridouane and Hasnaoui [11] numerically studied the effect of surface radiation on multiple natural convection solutions in a square cavity partially heated from below. Singh and Venkateshan[12] have discussed the importance of surface radiation coupled with natural convection in side vented open top cavities. Sharma et al.[13] numerically investigated turbulent natural convection in an enclosure partially heated from below. Oztop and Abu-Nadu[14] have numerically investigated the natural convection in partially heated enclosures filled with nanofluids.

While much progress has been accomplished in understanding flow and heat transfer in the closed cavities for combined natural convection and surface radiation, there are still some important areas requiring attention. However, to the best of my knowledge, average heat transfer coefficient for the hot portion of the bottom wall has not been examined in detail. In this study, the analysis of heat transfer has been investigated by placing centrally hot to full bottom hot walls and vertical walls as insulated and top horizontal wall as a cold wall of a cavity. The present investigation also focuses on development of an empirical correlation in terms of average convective Nusselt number which is the function of independent parameters like Rayleigh number, aspect ratio and hot bottom surface ratio.

MATHEMATICAL FORMULATION

The natural convection in a square cavity with having centrally heated from bottom shown schematically in Fig. 1, can be formulated as stream function and vorticity ($\omega - \psi$) form for a constant property fluid under the Boussinesq approximation, in non-dimensional form as

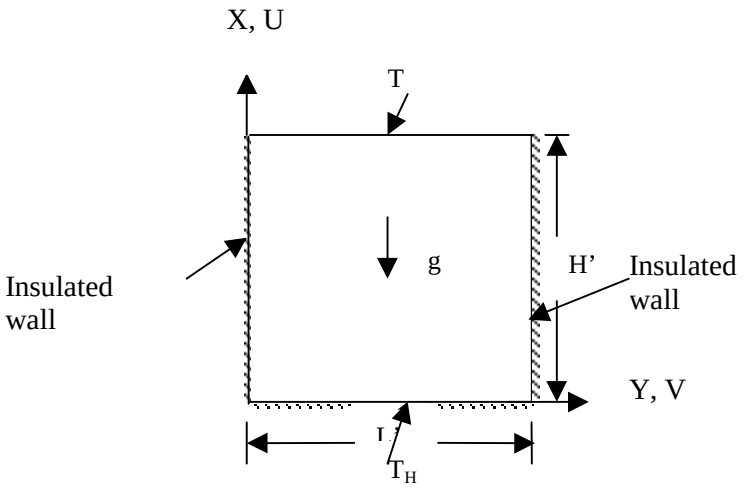

Fig. 1 Schematic of the physical system

$$U\frac{\partial \omega}{\partial X} + V\frac{\partial \omega}{\partial Y} = \Pr\left[\frac{\partial^2 \omega}{\partial X^2} + \frac{\partial^2 \omega}{\partial Y^2}\right] - Ra\ \frac{\partial \theta}{\partial Y} \quad (1)$$

$$\frac{\partial^2 \psi}{\partial X^2} + \frac{\partial^2 \psi}{\partial Y^2} = -\omega \times \Pr \quad (2)$$

$$U\frac{\partial \theta}{\partial X} + V\frac{\partial \theta}{\partial Y} = \left[\frac{\partial^2 \theta}{\partial X^2} + \frac{\partial^2 \theta}{\partial Y^2}\right] \quad (3)$$

$$U = \frac{\partial \psi}{\partial Y};\ V = -\frac{\partial \psi}{\partial X} \quad (4)$$

BOUNDARY CONDITIONS

The velocity boundary conditions are based on the assumption that the walls are rigid and impermeable and that the trapped air does not slip on the walls. In terms of stream function, this assumption can be translated to $\psi = 0$ at all the surfaces.

At the left and right vertical walls:

$$\psi = 0,\ \frac{1}{\Pr}\frac{\partial^2 \psi}{\partial Y^2} = -\omega \text{ and } \frac{\partial \theta}{\partial Y} = 0 \quad (5)$$

At the top of the horizontal wall of the cavity:

$$\psi = 0,\ \frac{1}{Pr}\frac{\partial^2 \psi}{\partial X^2} = -\omega \text{ and } \theta = 0 \qquad (6)$$

At the bottom of the adiabatic walls of the cavity:

$$\psi = 0,\ \frac{1}{Pr}\frac{\partial^2 \psi}{\partial X^2} = -\omega \text{ and } \frac{\partial \theta}{\partial X} = 0 \qquad (7)$$

At the centrally heated wall of the cavity:

$$\psi = 0,\ \frac{1}{Pr}\frac{\partial^2 \psi}{\partial X^2} = -\omega \text{ and } \theta = 1 \qquad (8)$$

METHOD OF SOLUTION

The governing equations (1) - (3) are first transformed into finite difference equations using a finite volume based finite difference method of Gosman et al [15]. Gauss - Seidel iterative procedure is used to solve the resulting algebraic equations. The details of solution procedure are available in Singh and Venkateshan [12]. A 41×41 non-uniform grid system for the computational domain is employed. The grid sizes have been fixed based on grid sensitivity analysis, the results of which are presented in the ensuing section in Table 1. A cosine function has been chosen to generate the grids in both along the X and Y directions in the cavity region. With reference to the implementation of derivative boundary conditions, three point formulae using second degree Lagrangian polynomial have been used. Upwinding has been used for representing the advection terms. The integrations required in all calculations are performed using Simpson's 1/3 rule for non-uniform step size. Under relaxation with a relaxation parameter of 0.5 was used for all three equations to obtain convergent results.

RESULTS AND DISCUSSION

Calculations have been made keeping in view the objective of evolving useful correlation for convective Nusselt number. Before proceeding further the result of a grid sensitivity study is presented.

GRID SENSITIVITY TEST

Table 1 shows the effect of the grid size on the $\overline{Nu_c}$ for a typical case with Ra = 1×10^6, A = 1, W = 1 and Pr = 0.7. It can be seen from Table 2 that the difference in $\overline{Nu_c}$ between the grid sizes of 41× 41 and 51× 51 is 0.277% which is the lowest. Thus grid pattern used in the present study is 41× 41.

Table 1 Grid independence study(Ra = 1×10^6, A = 1, W = 1 and Pr = 0.7)

m×n	$\overline{Nu_c}$	% change in $\overline{Nu_c}$
31× 31	17.177	-
41× 41	17.121	0.326
51× 51	17.138	0.277

Numerical code validation and comparison with benchmark results

The numerical code was extensively validated against the benchmark results of Ridouane and Hasnaoui [11] for pure natural convection, in terms of maximum and minimum of stream function values in a square cavity heated from below to check its validity as given in the next section for predicting the further results.

Comparison with streamline contours of present result with Ridouane and Hasnaoui[11]

Present results for typical values of various parameters are compared with numerical results of Ridouane and Hasnaoui[11] in trerms of streamlines and comparative results in terms of stream functions are given in the Table 2.

Table 2 Comparison of present results with Ridouane and Hasnaoui[11] in terms of stream function

Present result		Hasnaoui[11]		Present result		Hasnaoui[11]	
ψ_{max}	ψ_{min}	ψ_{max}	ψ_{min}	ψ_{max}	ψ_{min}	ψ_{max}	ψ_{min}
15	-15	13.39	-12.49	20	- 20	19.73	-

The above results show good agreement with the present results and results obtained by Ridouane and Hasnaoui[11].

Typical results for closed cavities partially heated from below

Having validated the present code with previous studies available in the literature, a detailed parametric study has been undertaken. Typical results from this study are presented here for a closed cavity partially heated from below. The parameters set is taken as Ra =1×10^3 - 3×10^6, A = 1-3, W = 0.25 - 1 and Pr = 0.7.

Streamline and isotherm patterns for closed cavities

Fig. 2 and Fig. 3 showing the streamlines (on left side) and isotherm lines (right side) corresponding to the given set of parameters as mentioned against figure captions indicate the influence of Rayleigh number. For Ra = 5×10^3, streamlines of Fig. 2 shows that the flow is organized in a single vortex

$\psi_{max} = -1, \psi_{min} = -3$

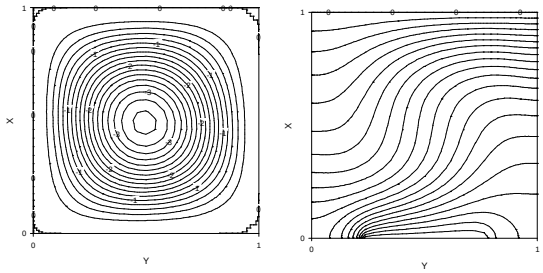

Fig. 2 Streamline (left) and isotherm patterns (right) for Ra = 5×10^3 , A =1, W = 0.5

$\psi_{max} = -1, \psi_{min} = -6$

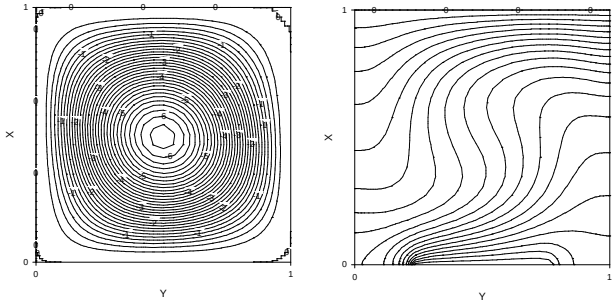

Fig. 3 Streamline (left) and isotherm patterns (right) for Ra = 1×10^4, A =1, W = 0.5

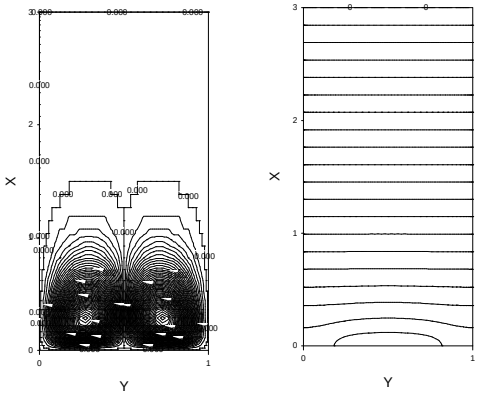

For left Figure

$\psi_{max} = 0.006$

$\psi_{max} = -0.006$

For right Figure

$\psi_{max} = 15$

$\psi_{max} = -15$

Fig. 4 Streamline (left) and isotherm patterns (right) for Ra = 1×10^3 , A =3, W = 0.5

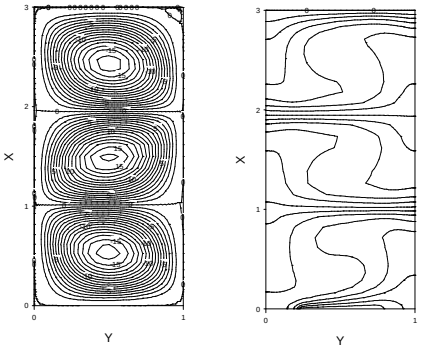

Fig.5 Streamline (left) and isotherm patterns (right) for Ra = 1×10^5, A =3, W = 0.5

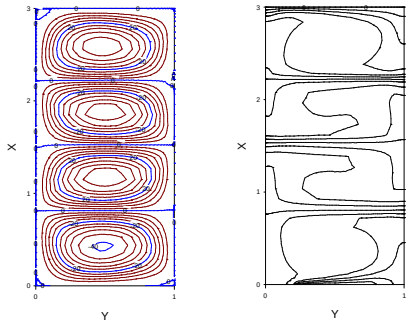

For left Figure

$\psi_{max} = 40$

$\psi_{max} = -40$

For right Figure

$\psi_{max} = 30$

$\psi_{max} = -30$

Fig. 6 Streamline (left) and isotherm patterns (right) for Ra = 1×10^6 , A =3, W = 0.5

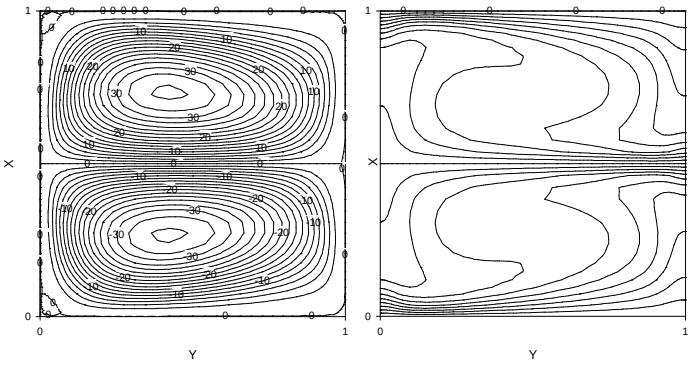

Fig. 7 Streamline (left) and isotherm patterns (right) for Ra = 1×10^6 , A =1, W = 1

rotating in the anti-clockwise direction. The corresponding isotherms show weak convection effect; they characterize a situation for which the conduction regime is still dominating. The vortex moves warm fluid from the hot element along the right insulated vertical wall, which results in higher temperature gradients at the right part of the cavity. At slightly higher Ra, Fig. 3 shows, for Ra =1×10^4, that the increase of Ra leads to the appearance of higher value of ψ in the core of the cavity. High temperature gradients are obtained near the active walls whereas the vortex moves warm fluid from the hot element along the right insulated vertical wall, which results in higher temperature gradients at the right part.

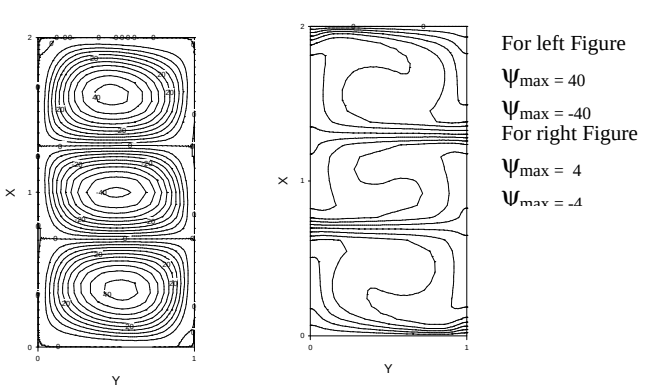

Fig. 8 Streamline (left) and isotherm patterns (right) for Ra = 1×10^6 , A =2, W = 1

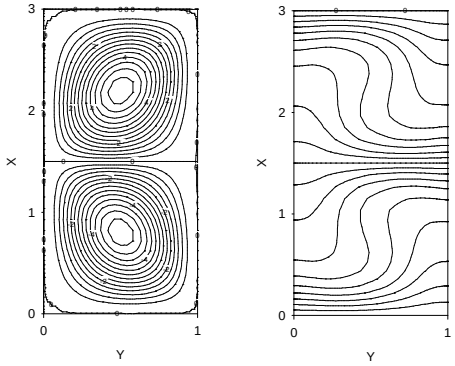

Fig. 9 Streamline (left) and isotherm patterns (right) for Ra = 3×10^4, A =2, W = 1

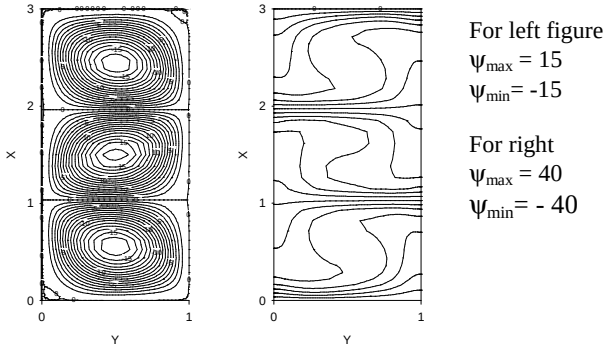

Fig. 10 Streamline (left) and isotherm patterns (right) for Ra = 1×10^5, A =3, W = 1

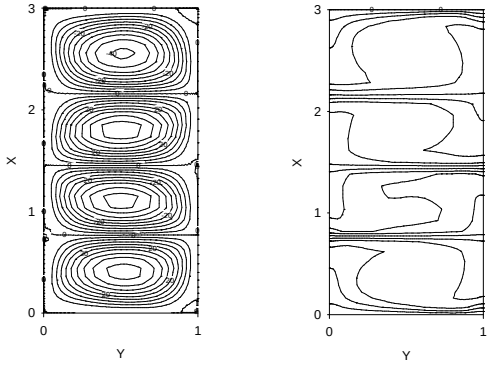

Fig. 11 Streamline (left) and isotherm patterns (right) for Ra = 3×10^6, A =3, W = 1

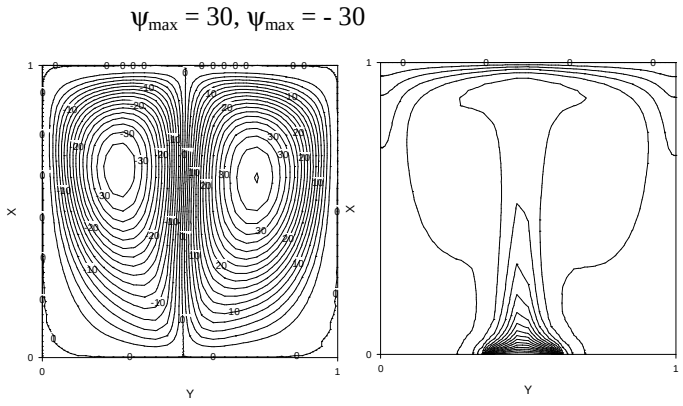

Fig. 12 Streamline (left) and isotherm patterns (right) for Ra = 1×10^6, A =1, W = 0.25

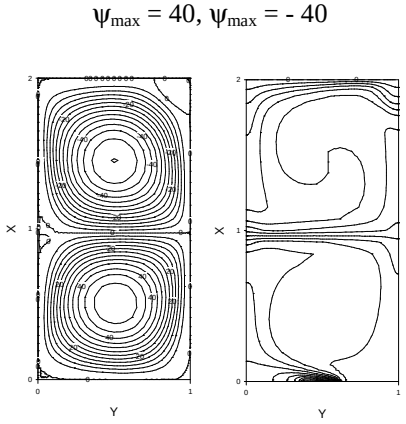

Fig. 13 Streamline (left) and isotherm patterns (right) for Ra = 1×10^6, A =2, W = 0.25

Fig. 4 and Fig. 5 show the streamlines and isotherm lines for the aspect ratio, A= 3 and W = 0.5 but for different Rayleigh numbers, Ra as mentioned with figure captions. For Ra = 1×10^3, streamlines of Fig. 4 indicates that the two symmetrical flow vortices are developed. The right vortex rotating in the clockwise direction, (ψ_{max} = 0.04) is the mirror image of the left vortex rotating in anti-clockwise direction (ψ_{min} = -0.04). The magnitude of stream function is very small and so the conduction dominant flow is present in the domain. Fig. 4 of the isotherm contours clearly indicates that the temperature lines

are flat and parallel from the bottom to top part of the cavity for aspect ratio, A = 3. For the same W = 0.5 and aspect ratio = 3 and for higher Ra = 1×10^5, streamlines of Fig. 5 shows the development of three vortices along the height due to convection heating of the fluid from the bottom to the top. The corresponding isotherm lines show that the heat is transferred from the heated element to the lower vortex, then from the lower vortex to the upper one, and finally from the latter to the cold wall as testified by the presence of the sharp gradients near the active walls and between the vortices.

Fig. 6 and Fig. 7 show the streamlines and isotherm lines for the parameters shown with corresponding figures. Fig. 7 of streamlines for Ra = 1×10^6, A =1, W = 1 shows that each vortex is in contact with only one active wall. The structure of the isotherms shows that the heat is transferred from the heated element to the lower vortex, then from the lower vortex to the upper one, and finally from the latter to the cold wall as testified by the presence of the sharp gradients near the active walls and between the vortices. In addition, the central part of each half of the cavity, containing the horizontal vortices, is isothermal. Fig. 6 of streamlines for Ra = 1×10^6, A =3, W = 0.5 indicates that four parallel vortices along the height of the cavity are developed. So as aspect ratio increases at higher Rayleigh number, more stratification loops are observed. In this case, each vortex is in contact with only one active wall. The isotherm lines are similar to the earlier case.

Fig. 8 and Fig. 9 show the streamlines and isotherm lines for the parameters shown with corresponding figures. Fig. 9 of streamlines for Ra = 3×10^4, A =2, W = 1 shows that two vortices are developed along the height of the cavity. Fig. 9 of isotherm lines are similar to the earlier case. However, Fig. 8 of streamlines for Ra = 1×10^6, A =2, W = 1 shows that development of three vortices along the height of the cavity. So it signifies that as Ra increases number of vortices also increases for the same aspect ratio and same portion of bottom heating.

Fig. 10 and Fig. 11 show the streamlines and isotherm lines for the parameters shown with figure captions. Fig. 10 of streamlines for Ra = 1×10^5, A =3, W = 1 indicates that three vortices are present in the domain along the height of the cavity. This is similar to the case for which Ra = 1×10^6, A =2, W = 1 as described in Fig. 8. The isotherm patterns are also observed similar to Fig. 8. However, the magnitudes of maximum and minimum stream function values, ψ_{max} and ψ_{min} are 15 and -15 respectively. The streamlines of Fig. 11 for the parameters Ra = 3×10^6, A =3, W = 1 indicates the development of four vortices along the height of the cavity. So it is clear that as Ra increases for the same aspect ratio and bottom-heating ratio, W the development of number of vortices along the height of the cavity increases. The development of isotherm lines is similar to the earlier cases.

Fig. 12 and Fig. 13 show of streamlines and isotherm lines for the parameters set as indicated with figure captions. The streamlines of Fig. 12 for Ra = 1×10^6, A =1, W = 0.25 indicates that the formation of two vortices along the width direction. In this case bottom-heating ratio is smaller than earlier cases and therefore heating amount to the adjacent fluid due to convection is small.

Streamlines and isotherms, obtained for relatively low and high Rayleigh numbers and W = 0.25, are presented in Fig. 14 and 15. For Ra = 1×10^3, A =1, W = 0.25, streamlines of Fig. 14 (on the left) show that the flow is organized in two vortexes i.e. the right primary vortex rotating in the clockwise direction is stronger than the left bottom corner secondary vortex. The maximum value of the stream function,ψ is 0.06 which shows conduction dominant flow. The corresponding isotherms (right side) show weak convection effect, they characterize a situation for which the conduction regime is still dominating. Near the heat source the isotherms show the influence of the natural convection but at the upper part of the cavity the isotherms become parallel to each other due to conduction effect.

Fig. 15 showing the streamlines and isotherms lines at higher Ra clearly indicates the affect of convection on the flow and

$\psi_{max} = 0.06$, $\psi_{min} = -0.02$ and in secondary vortex $\psi = -0.02$

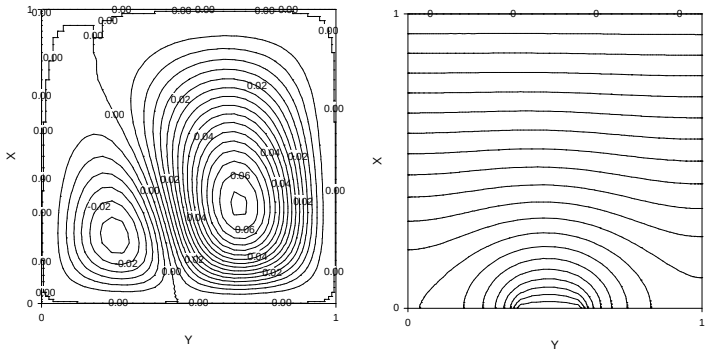

Fig. 14 Streamline (left) and isotherm patterns (right) for Ra = 1×10^3, A =1, W = 0.25

$\psi_{max} = 10$, $\psi_{min} = -10$

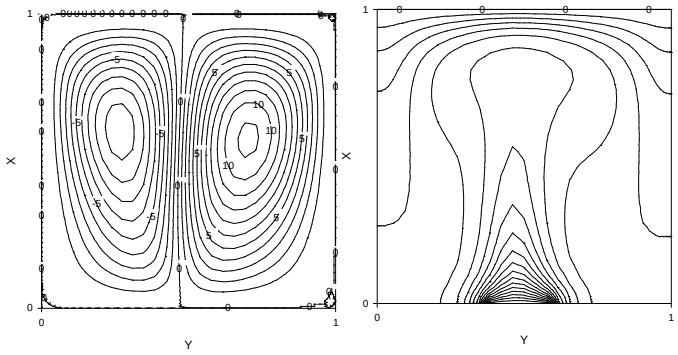

Fig. 15 Streamline (left) and isotherm patterns (right) for Ra = 1×10^5, A =1, W = 0.25

isotherm patterns. Streamlines (left side) show the development of two vortexes having ψ_{max} = 10 (right vortex) and ψ_{min} = -10 (left vortex). Isotherms (right side) clearly show the buoyancy effect on the flow.

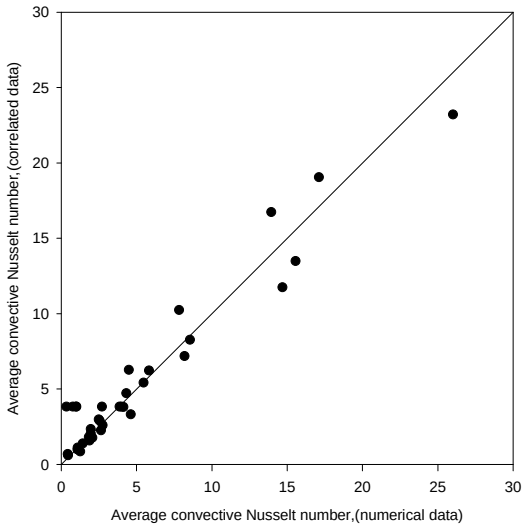

Fig. 16 Parity plot for average convectie Nusselt number for the range of parameters as shown in Table 1

CORRELATION

Based on a large set of numerical data (some 40 data sets in all), correlation for average convection Nusselt number has been derived as:

$$\overline{Nu}_c = 1.16\,Ra^{0.21}\,A^{-1.82}\,W^{0.20} \qquad (9)$$

As Rayleigh number directly affects convection heat transfer because power law form is used for Ra. The exponent of aspect ratio (A) is negative, which signifies $\overline{Nu}_c$ decreases with increase in aspect ratio. But the exponent of W is positive and hence as W increases, $\overline{Nu}_c$ also increases. A very high correlation coefficient of 0.991 and a standard deviation error of 0.129 indicate the goodness of the fit as shown in the parity plot of Fig.16.

CONCLUSIONS

Numerical results for laminar natural convection in an air-filled cavity having A = 1-3 partially heated from below are presented for wide ranges of Rayleigh number. Equations of momentum and energy have been solved using constant properties and Boussinesq approximations. As aspect ratio increases, the convection heat transfer decreases as obtained from correlation. As bottom heating ratio, W increases the convection heat transfer also increases. Average Nusselt number is greatly influenced by Rayleigh number as found from correlation. The number of vortices increases with increase in Rayleigh number in vertical direction.

REFERENCES

[1] Ostrach S., Natural Convection in Enclosures, ASME Journal of Heat Transfer, vol.110, 1988, pp. 1175 –1190.

[2] Hoogendoom. CJ., Natural Convection in Enclosures, Natural Convection in Enclosures, Proceedings of the 8th International Heat Transfer Conference, San Francisco, 1986, pp. 111 – 120.

[3] Vahl Davis G de., and Jones IP., Natural Convection in a Square Cavity, A Comparison Exercise, International Journal of Numerical Methods in Fluids, vol. 3, 1983, pp. 227 – 248.

[4] Akiyama M.,and Chong I.P., Numerical Analysis of Natural Convection with Surface Radiation in Square Enclosure, Numerical Heat Transfer, Part A, vol. 3, 1997, pp. 419 – 433.

[5] Mezrhab A., and Behir L., Radiation – Natural Convection Interactions in Partitioned Cavities, Int. J. Numerical Methods Heat Fluid Flow, vol. 9(1), 1999, pp. 186 – 203.

[6] Mahapatra SK., Sen S., and Sarkar A., Interaction of Surface Radiation and Variable Propert Natural Convection in a Differentially Heated Square Cavity – A Finite Element Analysis, Int. J.Numerical Methods Heat Fluid Flow, vol. 9(4), 1999, pp. 423– 443.

[7] Colomer G., Costa M., Consul R., and .Oliva A., Three Dimensional Numerical Simulation of Convect and Radiation in a Differentially Heated Cavity Using the Discrete Ordinate Method, Int. J. Heat Mas Transfer, vol. 47, 2004, pp. 257- 259.

[8] Hasnaoui M., Bilgen E., and Vasseur P., Natural Convection Heat Transfer in Rectangular Cavitie Partially Heated from Below, J. Thermo-Physics and Heat Transfer, vol. 6(2) ,1992, pp. 255-264.

[9] Ridouane EH., Hasnaoui M., Amahmid A., and Raji A., Interaction Between Natural Convection and Radiation in a Square Cavity Heated from Below, Numerical Heat Transfer-Part A, vol. 45, 2004, pp. 289-311.

[10] Ridouane EH., Hasnaoui M ., and Campo A., Effects of Surface Radiation on Natural Convection in a Rayleigh – Benard Square Enclosure Steady and Unsteady Conditions, Heat and Mass Transfer, vol. 42,,2006, pp. 214-225.

[11] Hassan EI., Ridouane EH., and Hasnaoui M, Effect of Surface Radiation on Multiple Natural Convection Solutions in a Square Cavity Partially Heated from Below, ASME J. Heat Transfer, vol. 128, 2006, pp. 1012-1021.

[12].Singh SN., and Venkateshan SP., Numerical Study of Natural Convection with Surface Radiation in Side-Vented Open Cavities, Intl. J. Thermal Sciences, vol. 43, 2004, pp. 865-876.

[13] Sharma A.K., Velusamy K.,and Balaji C.M,, Turbulent natural convection in an enclosure with localized heating from below, International Journal of Thermal Sciences, Vol.46,2007, pp.1232-1241.

[14] Oztop H F., and Abu-Nada E., Numerical study of natural convection in partially heated rectangular enclosures filled with nanofluids, International Journal of Heat and Fluid Flow, vol.29,2008,pp.1326-1336.

[15] A.D. Gosman, Pun W.M. Runchal, A.K. Spalding and D.B. Wolfshtein, Heat and Mass Transfer in Recirculating Flows, Academic Press, London, 1969.